Contents lists available at ScienceDirect

Digital Chinese Medicine

journal homepage: http://www.keaipublishing.com/dcmed

Differential expression profiles analysis of DNA methylation between "disease" and "syndrome" in coronary heart disease-induced unstable angina patients with Qi deficiency and blood stasis syndrome

WU Huaying[a], HU Hongchun[a], LIU Yufeng[a], LI Liang[b], LI Jing[b], HAN Yuming[c], XIAO Changjiang[c*], PENG Qinghua[b*]

a. School of Medicine, Hunan Normal University, Changsha, Hunan 410013, China

b. Provincial Key Laboratory of TCM Diagnostics, Hunan University of Chinese Medicine, Changsha, Hunan 410208, China

c. Department of Cardiology, Affiliated Hospital of Hunan Academy of Traditional Chinese Medicine, Changsha, Hunan 410006, China

ARTICLE INFO

Article history
Received 15 September 2023
Accepted 29 November 2023
Available online 25 December 2023

Keywords
Coronary heart disease (CHD)
Qi deficiency and blood stasis syndrome
Unstable angina pectoris
DNA methylation
Epigenetics
850K methylation chip

ABSTRACT

Objective To explore the differential expression profiles of DNA methylation sites/regions and potential molecular mechanisms in the peripheral blood of coronary heart disease (CHD)-induced unstable angina pectoris patients with or without Qi deficiency and blood stasis syndrome, and to provide scientific evidence for the conbination of disease and syndrome.

Methods According to the pre-determined inclusion and exclusion criteria, the study subjects were enrolled and divided into two groups namely CHD-induced unstable angina group (G group) and healthy control group (J group) to conduct "disease" analysis, while G group was further divided into Qi deficiency and blood stasis syndrome group (case group) and non-Qi deficiency blood stasis syndrome group (control group) to perform "syndrome" analysis. The general data and clinical information of the study subjects were collected. The peripheral venous blood was extracted on an empty stomach, and the Illumina Infinium MethylationEPIC BeadChip (850K methylation chip) was used to detect the differential expression profiles of DNA methylation in each group, ChAMP software (V 2.14.0) was used for the differential methylation data analysis, with a threshold of the adjusted *P* value (adj.*P*.val) < 0.01. Gene Ontology (GO) and Kyoto Encyclopedia of Genomes (KEGG) were employed for the functional and pathway enrichment analyses of related mapped genes.

Results A total of 263 differentially methylated CpG positions (DMPs) were screened out between G and J groups, including 191 hypermethylated positions such as cg05845204 and cg08906898, and 72 hypomethylated positions such as cg26919182 and cg13149459. These positions were mainly mapped to 148 genes encompassing RNA binding motif protein 39 (*RBM39*), acetyl-CoA acyltransferase 2 (*ACAA2*), protein phosphatase 1 regulatory subunit 12B (*PPP1R12B*), and the dual-specificity tyrosine phosphorylation-regulated kinase 2 (*DYRK2*). GO functional enrichment analysis revealed that the genes of the DMPs were primarily enriched in protein localization to chromosomes, regulation of cell morphogenesis, negative regulation of calcium-mediated signals, etc. KEGG pathway analysis suggested that the genes were mainly enriched in fatty acid metabolism and endocytosis pathways. In addition, a total of 23 differential methylation regions (DMRs) were identified, with overlapping

*Corresponding author: PENG Qinghua, E-mail: pqh410007@126.com. XIAO Changjiang, E-mail: changjiangx@163.com.

Peer review under the responsibility of Hunan University of Chinese Medicine.

DOI: 10.1016/j.dcmed.2024.01.008

Citation: WU HY, HU HC, LIU YF, et al. Differential expression profiles analysis of DNA methylation between "disease" and "syndrome" in coronary heart disease-induced unstable angina patients with Qi deficiency and blood stasis syndrome. Digital Chinese Medicine, 2023, 6(4): 451-466.

genes such as transmembrane protein 232 (*TMEM232*), ribosomal protein large P1 (*RPLP1*), peroxisomal biogenesis factor 10 (*PEX10*), and forkhead box N3 (*FOXN3*) recognized. It was found that GO functions were mainly enriched in the negative regulation of Ras protein signal transduction, small GTPase-mediated signal transduction, negative regulation, etc. A total of 1 703 differential methylation sites were screened out between case and control groups, including 444 increased methylation positions such as cg05573767 and 1 259 decreased methylationpositions such as cg19938535, and cg03893872. These positions were mapped to 1 108 genes such as ribosomal protein S6 kinase A2 (*RPS6KA2*), leucine rich repeat containing 16A (*LRRC16A*), and hedgehog acyltransferase (*HHAT*). According to the GO functional enrichment analysis, the genes relating to the DMPs were mainly enriched in biological functions such as transmembrane receptor protein serine/threonine kinase signaling pathway and axonogenesis. The KEGG pathway enrichment analysis suggested the involvement of Rap1 signaling pathway, adenosine 5'-monophosphate-activated protein kinase (AMPK) signaling pathway, etc. A total of 21 DMRs were identified, including 22 overlapping genes such as mucin 4 (*MUC4*), three prime repair exonuclease 1 (*TREX1*), and LIM homeobox 6 (*LHX6*). GO analysis demonstrated that the genes primarily participated in molecular functions such as positive regulation of transmembrane transport, regulation of fatty acid metabolism, and copper ion binding.

Conclusion This study reveals the methylation patterns of DMPs and DMRs in patients with Qi deficiency and blood stasis syndrome caused by CHD-induced unstable angina pectoris. Potential epigenetic regulation of fatty acid metabolism, Rap1 signaling, and other molecular functions are involved in the development of CHD between the "disease" and "syndrome".

1 Introduction

Coronary heart diseases (CHD) refer to heart failure caused by atherosclerosis in the coronary arteries which induces lumen stenosis or occlusion, leading to myocardial ischemia, hypoxia, or necrosis. It stands as a predominant factor contributing to global mortality and morbidity [1]. With the rapid social economic development, shifts in lifestyle and an aging population in China, the incidence and mortality rates of CHD continue to rise annually [2]. Report has pointed out that China has the highest mortality rate in cardiovascular disease, accounting for more than 40% of deaths from the disease [3]. Unstable angina pectoris is a common type of acute coronary syndromes, signifying a significant and severe clinical manifestation of CHD. It is characterized by sudden onset and easy recurrence, seriously affecting people's health and threatening their life.

Epigenetics is a genetic phenomenon centered on the inheritance of DNA methylation expression profiles, chromatin structural states, and gene expression profiles among cells, all without altering the underlying DNA sequence. Epigenetics regulate genetic expression mainly through DNA methylation, histone modifications, and non-coding RNA regulation [4]. The role of epigenetics in the pathophysiology of CHD has received ever-increasing attention, hence a comprehensive understanding of the disease becomes urgent. Epigenetic modifications are highly responsive to environmental risk factors related to CHD. Throughout the formation of atherosclerotic plaques, extensive epigenetic changes occurred in the homeostasis of endothelial cells or vascular smooth muscle cells [5]. As a highly conserved epigenetic modification, DNA methylation exerts important impacts on the stability, expression, and development of genes by covalent binding of a methyl group to cytosine, producing 5-methylcytosine (5mC) at the CpG dinucleotide site [6]. Studies confirmed the existence of global DNA methylation and gene-specific DNA methylation changes in CHD patients [7, 8].

Unstable angina pectoris induced by CHD falls into the "chest paralysis" and "heartache" categories in traditional Chinese medicine (TCM). The pathogenesis is attributed to deficiency in origin and excess in superficiality. The underlying deficiency is the deficiency of Qi, blood, Yin, and Yang, and is the excess of Qi stagnation, blood stasis, phlegm stasis, and cold coagulation. One epidemiological investigation on clinical syndrome distribution revealed that the Qi deficiency and blood stasis syndrome were common in CHD patients [9, 10]. TCM syndrome was a summary of a pathological state in a specific stage including the occurrence, development, and evolution of a disease, which was affected by congenital and acquired factors [11]. Using DNA methylation to conduct relevant research on TCM syndromes of CHD can provide new ideas for elucidating the essence of CHD syndromes from the pre-transcriptional level, and also a new perspective for finding specific biological targets in TCM syndromes. Therefore, in this study, we used the Illumina Infinium MethylationEPIC BeadChip (850K methylation chip) to explore the effect of DNA methylation on gene expression in CHD-induced unstable angina

pectoris patients with or without Qi deficiency and blood stasis syndrome, aiming to construct differential methylation expression profiles between "disease" and "syndrome", and to provide novel biomarkers for clinical research.

2 Materials and methods

2.1 Study participants

Participants diagnosed with unstable angina pectoris from December 1, 2019 to June 30, 2020 were recruited from the department of cardiology of the Affiliated Hospital of Hunan Academy of Traditional Chinese Medicine. Diagnosis and syndrome differentiation were conducted by a chief physician and two attending physicians, who had classified the enrolled patients into Qi deficiency and blood stasis syndrome and non-Qi deficiency blood stasis syndrome. Simultaneously, healthy volunteers undergoing physical examinations at the same hospital were recruited as controls. The study received approval from the Ethics Committee of the Affiliated Hospital of Hunan Academy of Traditional Chinese Medicine (20191119).

2.2 Diagnostic criteria

2.2.1 Western diagnostic criteria The guidelines outlined in the "Guidelines for the Diagnosis and Treatment of Unstable Angina and non-ST-segment Elevation Myocardial Infarction" by the Chinese Society of Cardiology [12] and the diagnostic criteria for unstable angina in the *Internal Medicine* [13], a 12th Five-Year Plan General Higher Education Undergraduate National Planning Textbook (8th edition), were adapted in the study. The grading of angina severity followed the rules established by the Canadian Cardiovascular Society (CCS), with grade I suggesting no limitation to normal physical activities such as walking and going upstairs, and angina occurs only during strenuous, rapid, or prolonged exertion; grade II signifyies slight limitation to ordinary physical activities, and angina occurs with fast walking, after meals, in cold or windy conditions, under emotional stress, or within a few hours of waking, and generally restricted when walking on flat ground for more than 200 m or climbing no less than one flight of stairs; grade III suggests marked limitation to ordinary physical activities, and angina occurs when walking on flat ground for less than 200 m or climbing only one flight of stairs; and grade IV suggests the occurrence of angina when engaging in even minimal physical activities or even at rest.

2.2.2 TCM diagnostic criteria In accordance with the "Syndrome Diffrentiation and Diagnostic Criteria for the Main Syndrome Types of Coronary Heart Disease and Angina Pectoris" as outlined by the Cardiology Branch of the Chinese Association of Traditional Chinese Medicine [14], various scores were designated for syndrome differentiation. The main syndromes include (A) Qi deficiency [(i) chest tightness or pain induced by exertion: 4 points; (ii) fatigue: 3 points; (iii) lassitude: 3 points; (iv) shortness of breath: 3 points; (v) spontaneous sweating: 3 points], and (B) blood stasis [(i) fixed chest pain with dark purple lips and nails: 4 points; (ii) the tongue in dark purple or presented petechiae and ecchymosis: 4 points; (iii) the sublingual veins in dark purple: 3 points; (iv) facial complexion in dark purple: 3 points; (v) the body produced petechiae or ecchymosis: 3 points]. At least one item from A and one from B should be identified during syndrome differentiation, with a total score of no less than 8 points signifying the presence of Qi deficiency and blood stasis syndrome.

2.3 Inclusion and exclusion criteria

2.3.1 Inclusion criteria for patients Patients were eligible if (i) both their biological parents were from Han ethnicity; (ii) they were between 40 and 80 years old; (iii) they were confirmed with unstable angina induced by CHD, with angina severity grading between I and III; (iv) they must meet both the western medicine and TCM diagnostic criteria of Qi deficiency and blood stasis syndrome, and for patients without the syndrome, they must meet the western medicine diagnostic criteria; (v) they were willing to sign an informed consent form.

2.3.2 Inclusion criteria for healthy controls Healthy controls were enrolled if (i) both their biological parents were from Han ethnicity; (ii) they were aged between 40 and 80 years old; (iii) they were in good physical health, without a history of major diseases or infectious diseases; (iv) their levels of blood routine, blood glucose, blood lipids, liver and kidney function, electrocardiogram, and cardiac ultrasound were all normal; (v) they were willing to sign an informed consent form.

2.3.3 Exclusion criteria Individuals were excluded if (i) they did not meet the diagnostic criteria; (ii) their age was less than 40 or over 80 years old; (iii) they were non-Han ethnicity minority population; their angina severity was graded as IV; (iv) they had severe health conditions such as congestive heart failure, severe arrhythmias, coronary spasms, valvular heart disease, or cardiogenic shock; (v) they had severe liver or kidney dysfunction, primary diseases in the blood system, mental illnesses, infectious disease, or malignant tumors.

2.4 Clinical information collection

The general information and clinical data of all participants, including age, gender, medical history, family history of inherited disease, medication history, blood routine, blood glucose, blood lipids, and liver and kidney function, were collected.

2.5 Specimen collection

Patients were subjected to fasting blood within 24 h after enrollment. Healthy controls underwent fasting blood in the morning on the second day after confirmation of inclusion (water fasting for at least 6 h), and 4 mL of venous peripheral blood was extracted and placed in ethylene diamine triacetic acid K2 (EDTA-K2) anti-coagulant tubes. The anti-coagulant tubes were gently inverted several times, and then aliquoted into 2 mL eppendorf (EP) tubes. The specimens were stored at – 80 °C and promptly subjected to DNA methylation detection.

2.6 DNA sample quality

DNeasy Blood & Tissue Kit (Qiagen, Germany) was used to isolate DNA from the peripheral blood. After DNA extraction, the NanoPhotometer NP60 UV spectrophotometer (Implen, Germany) was used to assess the purity and concentration of DNA. The genomic DNA meeting the following criteria was considered a qualified sample: (i) total amount $\geqslant$ 0.5 μg; (ii) concentration > 10 ng/μL; (iii) purity: optical density (OD) 260/280 value from 1.6 to 2.2, without protein or RNA contamination.

2.7 DNA methylation chip detection

The 850K methylation chip was used for sample detection. Eleven types of internal controls, including staining controls, extension controls, hybridization controls, target removal controls, bisulfite-conversion controls (I and II), specificity controls (I and II), non-polymorphic controls, negative controls, and restoration control, were utilized for quality control of each sample. The EZ DNA Methylation Gold Kit (Zymo Research, USA) was employed for bisulfite conversion, following the manufacturer's standard procedures. Approximately 500 ng of genomic DNA from each sample was used for the conversion with sodium bisulfite. The processed samples underwent DNA amplification and incubation, DNA fragmentation, precipitation, re-suspension, BeadChip hybridization, and were then transferred to the wash rack for cleaning. Subsequently, extension, staining, and iScan chip scanning were performed following the illumina iScan system (Illumina, USA) operating instructions.

2.8 DNA methylation chip data analysis

2.8.1 Data quality control The original idat files from EPIC were loaded, and the probe sites were filtered based on the following principles: (i) filtering out probes with $P \geqslant 0.01$; (ii) filtering out probes where the number of beads was less than 3 in over 5% of the samples; (iii) filtering out non-CpG probes included in the dataset; (iv) filtering out multi-hit probes; (v) filtering out probes associated with single nucleotide polymorphisms (SNPs) within 5 bp of CpG sites; (vi) filtering out probes on chromosomes X and Y.

2.8.2 Analysis of differentially methylated CpG positions (DMPs) Participants were divided into two groups namely CHD-induced unstable angina group (G group) and healthy control group (J group) to conduct "disease" analysis. Additionally, the unstable angina group was further divided into Qi deficiency and blood stasis syndrome group (case group) and non-Qi deficiency blood stasis syndrome group (control group) to perform "syndrome" analysis. The β-values of each group were compared, and the inter-group difference in β-values ($\Delta\beta$-values) was obtained to identify DMPs. The overall differences in DMPs between groups were visualized using R language (V 3.6.1) to generate volcano plots, heatmaps, and other visualizations. After obtaining normalized β-values, the ChAMP package (V 2.14.0) was employed. This function utilized linear regression and moderated t tests from the limma package (V 3.40.6) to conduct DMPs analysis between groups. The analysis included calculating the P value for each DMP, followed by multiple hypothesis testing to obtain the adjusted P value (adj.P.val). The threshold for selecting DMPs in this study was adj.P.val < 0.01 [15].

2.8.3 Analysis of differentially methylated regions (DMRs) In the genome, DMPs often cluster together, forming DMRs. The range of these regions can vary from a few hundred base pairs to megabases, and DMRs are believed to play a crucial role in gene imprinting regulation. To identify and analyze DMRs, the ChAMP package (V 2.14.0) was employed. The criteria for selecting DMRs were as follows: the region must contain more than 7 CpG sites, adjacent sites should be within 1 000 bp, and the false discovery rate (FDR) should be less than 0.05 [16].

2.8.4 Analyses of Gene Ontology (GO) and Kyoto Encyclopediaof Genes and Genomes (KEGG) enrichment The clusterProfiler package (V 3.12.0) was utilized for conducting GO and KEGG pathway enrichment analyses on the data obtained from DMPs and DMRs. The threshold for significance was set at $P < 0.05$.

2.9 Statistical analysis

SPSS 23.0 software was used to perform statistical analysis on clinical data. Continuous variables that met the normality test were expressed as mean ± standard deviation (SD), and those did not meet the normality test were expressed as median (interquartile range). Normal distribution analysis was performed on the data. Continuous variables that met the normality test underwent independent sample t test. Continuous variables that did not meet the normality test used Mann-Whitney U test in the non-parametric test. Chi-square test was used for categorical variables. Fisher's precision probability test was used for 2 × 2 contingency table statistic analysis. $P < 0.05$ was considered as a statistically significant.

3 Results

3.1 Basic information and clinical characteristics

A total of 17 CHD-induced unstable angina pectoris patients were enrolled in G group, and additional 17 healthy volunteers were recruited in J group. An analysis was conducted on the basic information and clinical characteristics of G and J groups (Table 1). In terms of age, G group exhibited a significantly higher average compared with J group (P < 0.001). No statistically significant differences in gender were observed between the two groups (P = 0.085). Regarding medical history, J group had no cases of hypertension, hyperlipidemia, or diabetes, whereas G group included 10 patients with hypertension (P < 0.001), 5 with hyperlipidemia (P = 0.044), and 5 with diabetes (P = 0.044). Peripheral blood tests revealed no significant differences in the levels of white blood cells (WBC), red blood cells (RBC), platelets (PLT), and hematocrit (Hct) between the two groups (P = 0.336, P = 0.314, P = 0.433, and P = 0.449, respectively). Liver function analysis indicated significantly elevated levels of aspartate aminotransferase (AST) in G group compared with J group (P = 0.001), while alanine aminotransferase (ALT) levels showed no significant difference (P = 0.073). Kidney function markers, including uric acid (UA) and creatinine (CRE) were notably higher in G group (P = 0.003 and P < 0.001, respectively). Fasting blood glucose (GLU) levels exhibited no significant differences between the two groups (P = 0.089). In terms of lipid profile, triglyceride (TG) levels were significantly higher (P = 0.007), high-density lipoprotein cholesterol (HDL-C) was significantly lower (P < 0.001) in G group than those in J group, while total cholesterol (TC) and low-density lipoprotein cholesterol (LDL-C) levels did not differ significantly (P = 0.521 and P = 0.375, respectively).

A total of 17 patients with CHD-induced unstable angina pectoris were divided into case group (n = 7) and control group (n = 10). There were no statistically significant differences in age and gender between the two groups (P = 0.180 and P = 0.661, respectively). A statistical analysis of blood test indicators revealed no significant differences in WBC, RBC, PLT, Hct, AST, ALT, UA, CRE, TG, HDL-C, LDL-C, and D-Dimer between the two groups (P > 0.05) . However, the activated partial thromboplastin time (APTT) level in case group was significantly higher than that in control group (P = 0.020) (Table 2).

3.2 Quality control of DNA sample

Following the extraction of DNA from the 34 experimental subjects, quality checks were performed to assess the integrity of genomic DNA in accordance with established quality standards. The experimental results revealed that all samples met the required standards. Subsequently, probe-based detection was conducted on all samples at designated loci, revealing that the detection rates for all samples exceeded 99%. This indicated that all samples met the experimental requirements and were qualified for subsequent experiments (Table 3).

3.3 DMPs screening results

3.3.1 DMPs associated with unstable angina pectoris in CHD patients DMPs play a crucial role in methylation studies, particularly in identifying potential biomarkers. In comparison with J group, a total of 263 DMPs associated with "disease" in G group were screened out (adj.P.val < 0.01). Among them, there were 191 hypermethylated sites and 72 hypomethylated sites. The visualization of DMPs was presented through heat maps and volcano plots (Figure 1 and 2). Based on the $\Delta\beta$-values, specific sites such as cg05845204, cg12691488, and cg00500229 showed increased methylation (Table 4), while sites like cg04462931, cg26919182, and cg09516963 demonstrated decreased methylation (Table 5).

Table 1 Comparison of general data and clinical characteristics between G and J groups

Group	Age (years)	Gender		Hypertension		Hyperlipidemia		Diabetes		WBC (10^9/L)	RBC (10^{12}/L)	PLT (10^9/L)
		Male	Female	Yes	No	Yes	No	Yes	No			
G group (n=17)	63 (12)	11	6	10	7	5	12	5	12	6.13 (1.53)	4.43 ± 0.53	184.47 ± 53.39
J group (n=17)	46.53 ± 4.50	5	12	0	17	0	17	0	17	5.75 ± 1.57	4.26 ± 0.40	197.20 ± 33.48
P value	< 0.001[a]	0.085[a]		< 0.001[b]		0.044[b]		0.044[b]		0.336[a]	0.314[c]	0.433[c]

Group	Hct (%)	AST (U/L)	ALT (U/L)	UA (μmol/L)	CRE (μmol/L)	GLU (mmol/L)	TG (mmol/L)	TC (mmol/L)	HDL-C (mmol/L)	LDL-C (mmol/L)
G group (n=17)	39.45 ± 4.47	36.10 (19.80)	12.80 (13.60)	325.07 ± 83.83	73.34 ± 17.03	5.64 (1.05)	1.26 ± 0.55	4.32 (0.81)	1.09 (0.16)	2.56 (0.54)
J group (n=17)	38.38 ± 3.18	18.67±6.51	15.17 ± 7.48	248.40 ± 38.03	54.81 ± 6.42	5.22 ± 0.31	0.81 ± 0.24	4.22 ± 0.53	1.59 ± 0.16	2.64 ± 0.48
P value	0.449[c]	0.001[a]	0.073[a]	0.003[c]	< 0.001[c]	0.089[a]	0.007[c]	0.521[a]	< 0.001[a]	0.375[a]

Continuous variables with normal distribution were presented as mean ± SD, while those not conforming to normal distribution were expressed as median (interquartile range). [a] Non-parametric test, [b] Chi-square test, [c] t test. WBC, white blood cell. RBC, red blood cell. PLT, platelet. Hct, hematocrit. AST, aspartate aminotransferase. ALT, alanine aminotransferase. UA, uric acid. CRE, creatinine. GLU, blood glucose. TG, triglyceride. TC, total cholesterol. HDL-C, high-density lipoprotein cholesterol. LDL-C, low-density lipoprotein cholesterol.

Table 2 Comparison of clinical data between case and control groups

Group	Age (years)	Gender		WBC (10^9/L)	RBC (10^{12}/L)	PLT (10^9/L)	Hct (%)	AST (U/L)	ALT (U/L)
		Male	Female						
Case group (n = 7)	67.17 ± 6.01	4	3	6.67 ± 2.21	4.22 (0.88)	156.67 ± 24.29	38.22 ± 3.80	26.36 ± 6.76	18.65 ± 7.32
Control group (n = 10)	63 (10)	7	3	5.95 ± 0.81	4.54 ± 0.55	199.64 ± 59.57	40.12 ± 4.84	35.15 ± 14.93	18.40 (27.30)
P value	0.180[a]	0.661[b]		0.808[c]	0.462[a]	0.180[c]	0.462[c]	0.350[c]	0.591[a]

Group	UA (μmol/L)	CRE (μmol/L)	GLU (mmol/L)	TG (mmol/L)	TC (mmol/L)	HDL-C (mmol/L)	LDL-C (mmol/L)	APTT (s)	D-Dimer (mg/L)
Case group (n = 7)	327.42 ± 118.96	75.22 ± 16.85	5.21 (6.39)	1.36 ± 0.75	3.84 ± 0.95	1.07 ± 0.12	2.01 ± 0.79	35.60 (35.11)	0.88 ± 0.64
Control group (n = 10)	323.79 ± 64.51	72.31 ± 17.85	5.71 ± 0.48	1.21 ± 0.44	4.61 (0.61)	1.11 (0.17)	2.57 (0.36)	28.30 (3.10)	0.35 (1.36)
P value	1.000[c]	1.000[c]	0.525[a]	0.733[c]	0.122[a]	0.660[a]	0.180[a]	0.020[a]	0.591[a]

Continuous variables conforming to normal distribution were presented as mean ± SD, while those not conforming to normal distribution were expressed as median (interquartile range). [a] Non-parametric test, [b] Chi-square test, [c] t test. APTT, activated partial thromboplastin time.

Table 3 Results of quality control and detection rate of the DNA samples

Sample	Concentration (ng/μL)	Volume (μL)	Amount (μg)	OD 260/280	Check out checkpoint	Detection rate	Quality control result
G-1	19.60	80	1.47	1.87	865 542	0.999 6	Eligible
G-2	11.20	80	0.84	2.06	865 575	0.999 6	Eligible
G-3	13.50	80	1.01	1.98	865 486	0.999 5	Eligible
G-4	12.30	80	0.92	2.07	865 098	0.999 1	Eligible
G-5	10.60	80	0.80	2.14	865 110	0.999 1	Eligible
G-6	15.90	80	1.19	2.08	865 002	0.998 9	Eligible
G-7	11.90	80	0.89	1.70	865 434	0.999 4	Eligible
G-8	14.30	80	1.07	2.11	864 925	0.998 9	Eligible
G-9	20.20	80	1.51	2.07	865 145	0.999 1	Eligible
G-10	13.00	80	0.97	2.04	865 500	0.999 5	Eligible
G-11	13.30	80	1.00	1.88	865 430	0.999 4	Eligible
G-12	11.50	80	0.86	2.19	865 385	0.999 4	Eligible
G-13	13.20	80	0.99	2.13	865 474	0.999 5	Eligible
G-14	16.70	80	1.25	2.08	865 415	0.999 4	Eligible
G-15	38.80	80	2.91	1.60	865 530	0.999 6	Eligible
G-16	32.80	80	2.46	1.96	865 183	0.999 2	Eligible
G-17	13.50	80	1.01	2.12	865 469	0.999 5	Eligible
J-1	13.40	80	1.00	1.98	865 209	0.999 2	Eligible
J-2	10.80	80	0.81	1.94	865 249	0.999 2	Eligible
J-3	17.50	80	1.31	1.66	865 165	0.999 1	Eligible
J-4	16.80	80	1.26	2.08	865 164	0.999 1	Eligible
J-5	20.60	80	1.54	1.94	864 851	0.998 8	Eligible
J-6	18.00	80	1.35	1.70	865 156	0.999 1	Eligible
J-7	18.40	80	1.38	2.03	865 137	0.999 1	Eligible
J-8	12.60	80	0.94	2.16	865 120	0.999 1	Eligible
J-9	11.00	80	0.82	2.08	865 181	0.999 1	Eligible
J-10	56.60	80	4.25	1.77	865 146	0.999 1	Eligible
J-11	11.00	80	0.82	2.12	865 067	0.999 0	Eligible
J-12	13.00	80	0.97	2.07	864 940	0.998 9	Eligible
J-13	14.60	80	1.09	2.17	865 035	0.999 0	Eligible
J-14	11.40	80	0.85	1.64	865 255	0.999 2	Eligible
J-15	11.10	80	0.83	1.95	865 108	0.999 1	Eligible
J-16	51.00	80	3.83	1.72	865 207	0.999 2	Eligible
J-17	10.60	80	0.80	2.11	865 288	0.999 3	Eligible

These "disease"-associated DMPs were mapped to a total of 148 genes. Within the hypermethylated sites, 116 genes were identified, among which 103 were differentially expressed. These genes were primarily mapped to RNA binding motif protein 39 (*RBM39*), scaffold protein involved in DNA repair (*SPIDR*), acetyl-CoA acyltransferase 2 (*ACAA2*), and long intergenic non-protein coding RNA 644649 (*LOC644649*) based on the Δβ-values. In the hypomethylated sites, 55 genes were initially mapped, among which 45 were differentially expressed after removing duplicates. These genes were predominantly associated with rotein phosphatase 1 regulatory subunit 12B (*PPP1R12B*), the dual-specificity tyrosine phosphorylation-regulated kinase 2 (*DYRK2*), etc. (Table 6).

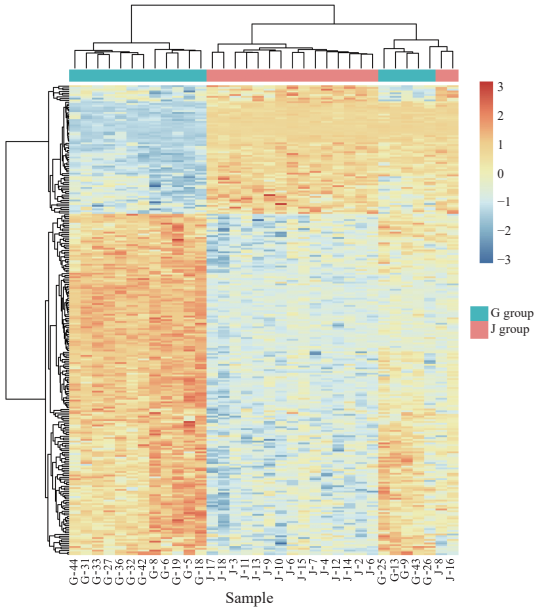

Figure 1 Heat map of CHD-induced unstable angina related DMPs

Color ranging from light to dark (approaching deep red or deep blue) indicates the degree of significant methylation from low to high in different samples.

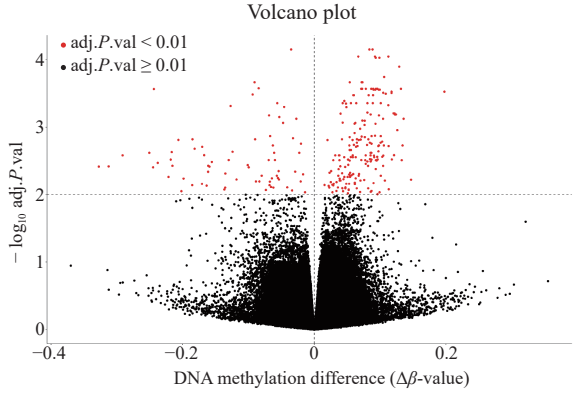

Figure 2 Volcano plot of DMPs in CHD-induced unstable angina patients

3.3.2 DMPs results associated with Qi deficiency and blood stasis syndrome in patients with CHD-induced unstable angina pectoris In comparison with control group, a total of 1 703 DMPs representing the "syndrome"

Table 4 The top 10 hypermethylated sites in CHD-induced unstable angina patients

CpG position	adj.*P*.val	Δβ-value	Chr	Gene
cg05845204	0.000 297 34	0.197 698 25	20	*RBM39*
cg12691488	0.005 970 21	0.147 038 74	1	—
cg00500229	0.000 748 57	0.135 712 12	1	—
cg04677840	0.001 859 50	0.134 138 76	17	—
cg09102486	0.003 072 86	0.132 928 18	5	—
cg19061000	0.000 269 80	0.131 734 82	14	—
cg08937153	0.000 126 64	0.129 084 67	8	*SPIDR*
cg17264064	0.001 102 66	0.126 137 65	18	*ACAA2*
cg14881054	0.000 646 63	0.124 006 95	7	—
cg04946709	0.000 646 63	0.122 593 53	16	*LOC644649*

Chr, chromosome number according to the reference genome GRCh37. —, no mapped gene.

Table 5 The top 10 hypomethylated sites in CHD-induced unstable angina patients

CpG position	adj.*P*.val	Δβ-value	Chr	Gene
cg04462931	0.003 820 67	− 0.327 379 5	7	—
cg26919182	0.003 792 68	− 0.312 476 3	1	*PPP1R12B*
cg09516963	0.002 605 35	− 0.291 207 6	12	*DYRK2*
cg13149459	0.002 393 35	− 0.250 677 9	1	*PPP1R12B*
cg00151744	0.003 915 36	− 0.244 940 8	15	—
cg23256579	0.000 272 11	− 0.243 741 2	12	*PRR4*
cg25343008	0.003 370 23	− 0.237 861 5	1	*PPP1R12B*
cg11955727	0.005 433 79	− 0.221 574 2	2	—
cg01966510	0.003 006 00	− 0.218 123 1	15	*UBE2Q2P1*
cg00063654	0.002 327 66	− 0.216 573 9	3	*RFTN1*

Chr, chromosome number according to the reference genome GRCh37. —, no mapped gene.

Table 6 The top 10 mapped genes on differentially methylated sites associated with CHD-induced unstable angina patients

Hyper gene	Δβ-value	Hypo gene	Δβ-value
RBM39	0.197 698 25	*PPP1R12B*	− 0.312 476 3
SPIDR	0.129 084 67	*DYRK2*	− 0.291 207 6
ACAA2	0.126 137 65	*PRR4*	− 0.243 741 2
LOC644649	0.122 593 53	*UBE2Q2P1*	− 0.218 123 1
MTFR1	0.120 410 69	*RFTN1*	− 0.216 573 9
ZNF607	0.117 399 99	*ZNF138*	− 0.215 514 4
PRKCI	0.117 351 57	*LOC101927502*	− 0.201 925 7
GABPA	0.113 122 07	*FAM35A*	− 0.185 517 6
LOC100128164	0.112 859 56	*TFDP1*	− 0.181 829 1
FOXN3	0.112 568 93	*ERV3-1*	− 0.170 655 6

Hyper gene, gene mapped to hypermethylated site. Hypo gene, gene mapped to hypomethylated site.

in case group were identified, comprising 444 hypermethylated sites and 1 259 hypomethylated sites. Visualization of these DMPs was presented through heat maps and volcano plots (Figure 3 and 4). Notable hypermethylated sites based on Δβ-values included cg01808030, cg05373962, and cg07959070 (Table 7). Hypomethylated sites included cg19585676, cg19938535, and cg17920646 (Table 8).

These DMPs were mapped to a total of 1 108 genes, with 302 genes initially identified from hypermethylated sites, of which 295 were differentially expressed genes after removing duplicates. For hypomethylated sites, 934 genes were initially mapped, of which 813 were differentially expressed genes after removing duplicates. Based on Δβ-values, hypermethylated sites were primarily associated with genes such as RIB43A domain with coiled-coils 2 (*RIBC2*), ribosomal protein S6 kinase A2 (*RPS6KA2*), and family with sequence similarity 118 member A (*FAM118A*), while hypomethylated sites were primarily associated with genes such as leucine rich repeat containing 16A (*LRRC16A*) and hedgehog acyltransferase (*HHAT*) (Table 9).

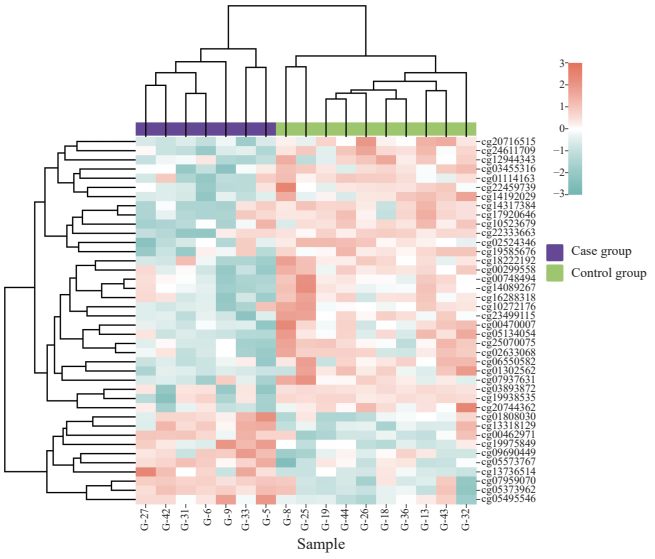

Figure 3 Heat map of DMPs associated CHD-induced Qi deficiency and blood stasis syndrome

Color from light to dark indicates the degree of significant methylation in different samples from low to high.

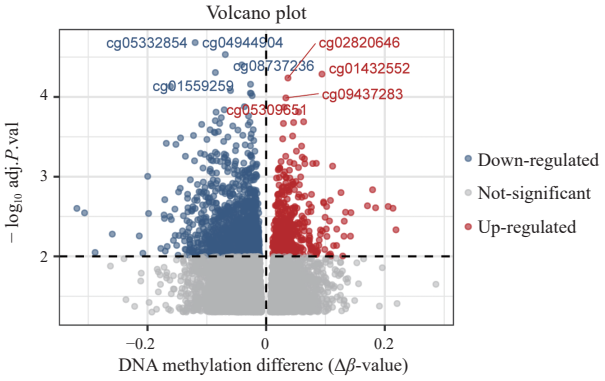

Figure 4 Volcano plot of DMPs associated with different syndrome of CHD-induced unstable angina pectoris

3.4 DMRs screening results

3.4.1 DMRs results associated with CHD-induced unstable angina pectoris In comparison with J group, a total of 23 DMRs associated with the "disease" in G group were identified. These DMRs were primarily located on 15 chromosomes, and genes overlapping with DMRs included transmembrane protein 232 (*TMEM232*), ribosomal protein large P1 (*RPLP1*), peroxisomal biogenesis factor 10 (*PEX10*), and forkhead box N3 (*FOXN3*) (Table 10).

Table 7 The top 10 hypermethylated sites in CHD-induced unstable angina patients with Qi deficiency and blood stasis syndrome

CpG position	adj.*P*.val	Δβ-value	Gene	Feat.cgi
cg01808030	0.004 619 6	0.218 758 3	*RIBC2*	Body-island
cg05373962	0.002 584 61	0.210 607	—	IGR-shore
cg07959070	0.002 446 61	0.202 859 4	*C22orf34*	Body-island
cg00462971	0.002 187 98	0.185 204 1	—	IGR-shore
cg05573767	0.002 057 31	0.182 692 1	*RPS6KA2*	Body-opensea
cg13318129	0.002 411 16	0.173 325 6	*FAM118A*	3'UTR-opensea
cg09690449	0.009 217 56	0.168 619 2	—	IGR-opensea
cg19975849	0.002 581 55	0.145 316 1	—	IGR-opensea
cg05495546	0.003 642 95	0.144 116 3	—	IGR-shore
cg13736514	0.001 673 40	0.136 815 7	—	IGR-opensea

Feat.cgi, methylated island region feature type. —, no mapped gene.

Table 8 The top 10 hypomethylated sites in CHD-induced unstable angina patients with Qi deficiency and blood stasis syndrome

CpG position	adj.*P*.val	Δβ-value	Gene	Feat.cgi
cg19585676	0.002 445 66	– 0.317 856 64	*HLA-A*	3'UTR-shore
cg19938535	0.002 744 72	– 0.306 245 23	*LRRC16A*	Body-opensea
cg17920646	0.008 893 58	– 0.288 288 26	—	IGR-island
cg14317384	0.005 229 12	– 0.259 337 81	—	IGR-island
cg12944343	0.005 957 17	– 0.210 106 38	—	IGR-opensea
cg03893872	0.008 835 45	– 0.207 630 99	*HHAT*	TSS1500-shore
cg00299558	0.001 014 39	– 0.198 130 16	*VWA5B2*	Body-shore
cg25070075	0.002 919 09	– 0.196 110 58	—	IGR-island
cg14089267	0.007 928 20	– 0.177 499 42	—	IGR-island
cg22333663	0.002 877 63	– 0.171 943 94	*MOCOS*	Body-shelf

Feat.cgi, methylated island region feature type. —, no mapped gene.

3.4.2 DMRs results associated with Qi deficiency and blood stasis syndrome in CHD-induced unstable angina pectoris In comparison with control group, a total of 21 DMRs in case group were identified, involving 22 overlapping genes. These DMRs were primarily located on 13 chromosomes, and the overlapped genes included mucin 4 (*MUC4*), prime repair exonuclease 1 (*TREX1*), and LIM hom eobox 6 (*LHX6*) (Table 11).

Table 9 The top 10 mapped genes on differentially methylated sites associated with CHD-induced unstable angina patients with Qi deficiency and blood stasis syndrome

Hyper gene	Δβ-value	Hypo gene	Δβ-value
RIBC2	0.218 758 3	*HLA-A*	– 0.317 856 64
C22orf34	0.202 859 4	*LRRC16A*	– 0.306 245 23
RPS6KA2	0.182 692 1	*HHAT*	– 0.207 630 99
FAM118A	0.173 325 6	*VWA5B2*	– 0.198 130 16
C9orf171	0.133 605	*MOCOS*	– 0.171 943 94
DFNA5	0.127 676 2	*PRSS22*	– 0.168 198 92
HAND2	0.123 142 4	*CUX2*	– 0.167 129 59
ZBTB44	0.118 667 5	*PEX5L*	– 0.166 224 65
PAX7	0.115 135 1	*ODZ4*	– 0.159 808 73
B3GAT1	0.114 019 8	*PCDHA2*	– 0.158 852 84

Hyper gene, gene mapped to hypermethylated site. Hypo gene, gene mapped to hypomethylated site.

3.5 GO enrichment analysis

3.5.1 GO enrichment analysis of DMPs associated with CHD-induced unstable angina pectoris In comparison between G and J groups, a total of 409 significantly different GO entries were identified ($P < 0.05$). Among these, 331 were related to biological process (BP), involving processes such as protein localization to the chromosome, regulation of cell morphogenesis, long-term synaptic depression, and negative regulation of calcium-mediated signaling. Additionally, 47 entries were associated with cellular component (CC), including compact myelin, neuron spine, side of the membrane, and cluster of actin-based cell projections. And 31 entries were linked to molecular function (MF), covering activities such as translation factor activity, glutamate receptor binding, receptor signaling complex scaffold activity, ionotropic glutamate receptor binding, and low-density lipoprotein particle receptor binding (Figure 5).

Table 10 DMRs related to CHD-induced unstable angina pectoris

Chr	Start	End	Min FDR	Mapping gene
Chr5	110 062 343	110 062 837	$8.630\,8 \times 10^{-37}$	*TMEM232*
Chr15	69 744 390	69 745 373	$6.047\,3 \times 10^{-33}$	*RPLP1*
Chr1	2 344 561	2 345 894	$1.513\,0 \times 10^{-24}$	*PEX10*
Chr14	89 878 374	89 879 153	$7.713\,6 \times 10^{-24}$	*FOXN3*
Chr19	33 210 166	33 210 851	$2.546\,5 \times 10^{-21}$	*TDRD12*
Chr13	114 291 735	114 292 740	$9.105\,1 \times 10^{-19}$	*TFDP1*
Chr15	69 755 217	69 755 745	$1.464\,1 \times 10^{-15}$	*RPLP1*
Chr10	29 698 152	29 699 147	$5.695\,7 \times 10^{-15}$	*PTCHD3P1*
Chr8	9 009 097	9 009 499	$1.079\,3 \times 10^{-14}$	*PPP1R3B*
Chr1	172 113 756	172 114 419	$2.239\,6 \times 10^{-12}$	*DNM3OS, MIR199A2*
Chr20	62 168 463	62 169 334	$5.346\,2 \times 10^{-12}$	*PTK6*
Chr21	42 797 488	42 798 199	$7.659\,9 \times 10^{-12}$	*MX1*
Chr4	187 422 005	187 422 343	$3.395\,4 \times 10^{-11}$	*F11-AS1, RNU6*
Chr5	68 628 240	68 628 856	$1.774\,6 \times 10^{-10}$	*CCDC125*
Chr19	8 273 643	8 274 283	$3.243\,8 \times 10^{-10}$	*CERS4*
Chr2	74 669 048	74 669 573	$3.404\,9 \times 10^{-10}$	*RTKN*
Chr2	95 830 912	95 831 116	$3.500\,3 \times 10^{-10}$	*ZNF2*
Chr7	32 339 054	32 339 497	$4.241\,1 \times 10^{-10}$	*PDE1C*
Chr19	16 830 287	16 830 859	$4.357\,6 \times 10^{-10}$	*NWD1*
Chr17	7 283 774	7 284 049	$4.597\,0 \times 10^{-10}$	*TNK1*
Chr20	3 218 331	3 218 579	$7.356\,7 \times 10^{-10}$	*SLC4A11*
Chr6	31 827 858	31 828 260	$7.659\,2 \times 10^{-10}$	—
Chr15	91 473 091	91 473 569	$7.829\,3 \times 10^{-10}$	*UNC45A*

Chr, chromosome number according to the reference genome GRCh37. Start, DMR start position. End, DMR end position. Min FDR, minimum FDR value. Mapping gene, overlapping genes. —, no mapped gene.

Table 11 DMRs information for Qi deficiency and blood stasis syndrome in CHD-induced unstable angina pectoris patients

Chr	Start	End	Width	Value	Mapping gene
Chr5	135 415 762	135 416 613	851	– 1.215 9	—
Chr3	195 489 708	195 490 309	601	– 1.085 8	*MUC4*
Chr3	48 507 354	48 507 618	264	– 0.962 5	*TREX1*
Chr9	124 989 052	124 990 276	1 224	– 0.771 8	*LHX6*
Chr6	30 039 175	30 039 801	626	– 0.636 4	—
Chr4	96 470 286	96 470 626	340	0.495 8	*UNC5C*
Chr7	122 526 408	122 526 940	532	0.498 4	*CADPS2*
Chr4	90 758 120	90 758 537	417	0.525 9	*SNCA*
Chr2	198 650 603	198 651 498	895	0.548 5	*BOLL*
Chr15	23 810 163	23 810 861	698	0.585 1	*RNF39*
Chr16	66 613 096	66 613 407	311	0.597 2	—
Chr1	153 599 479	153 600 156	677	0.633 8	*S100A13*、*S100A1*
Chr6	31 650 735	31 651 362	627	0.636 5	*LY6G5C*
Chr19	57 049 695	57 050 834	1 139	0.640 2	*ZFP28*
Chr19	57 182 816	57 183 342	526	0.641 7	*MKRN3, ZNF835*
Chr12	75 784 541	75 785 295	754	0.666 6	*GLIPR1L2, CAPS2*
Chr19	9 785 295	9 786 131	836	0.678 9	*ZNF562*
Chr13	110 438 906	110 439 453	547	0.691 4	*IRS2*
Chr21	35 831 954	35 832 204	250	0.786 4	*KCNE1*
Chr19	57 742 112	57 742 444	332	0.824 3	*AURKC*
Chr18	6 414 958	6 415 118	160	1.041 1	*CMTM2, L3MBTL4*

Chr, chromosome number according to the reference genome GRCh37. Start, DMR start position. End, DMR end position. Value, confidence indicator. Mapping gene, overlapping genes. —, no mapped gene.

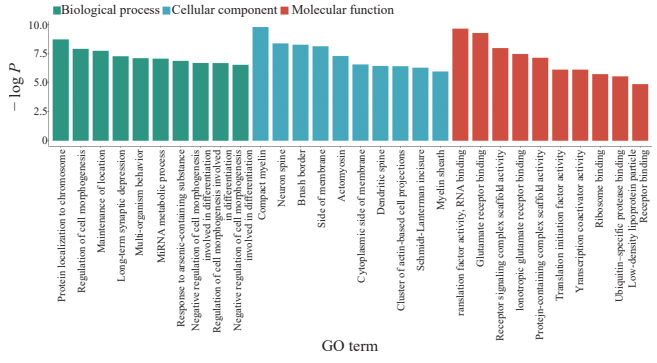

Figure 5 The top 10 GO enrichment of DMPs associated with CHD-induced unstable angina pectoris

3.5.2 GO enrichment analysis of DMPs associated with Qi deficiency and blood stasis syndrome in CHD-induced unstable angina pectoris In comparison between case and control groups, a total of 83 significantly different GO entries were identified ($P < 0.05$). Among these, 24 were related to BP, involving processes such as the transmembrane receptor protein serine/threonine kinase signaling pathway, axonogenesis, neuron projection guidance, and G protein-coupled glutamate receptor signaling pathway. Additionally, 38 entries were associated with CC, including stress fiber, contractile actin filament bundle, actin filament bundle, and cluster of actin-based cell projections. And 21 entries were linked to MF, covering activities such as actin binding, DNA-binding transcription factor binding, and transmembrane receptor protein tyrosine phosphatase activity (Figure 6).

3.5.3 GO enrichment analysis of DMRs associated with CHD-induced unstable angina pectoris In comparison between G and J groups, 152 significantly different GO entries related to DMRs genes were identified ($P < 0.05$). Among these, 123 were related to BP, including negative regulation of Ras protein signal transduction, negative regulation of small GTPase-mediated signal transduction, negative regulation of growth, and mitotic DNA damage checkpoint. Furthermore, 6 entries were associated with CC, involving integral component of peroxisomal membrane, intrinsic component of peroxisomal membrane, protein serine/threonine phosphatase complex, and phosphatase complex. Additionally, 23 entries were linked to MF, covering non-membrane spanning protein tyrosine kinase activity, GTP binding, purine ribonucleoside binding, and guanyl nucleotide binding. The top 10 entries for each GO category are displayed in Figure 7.

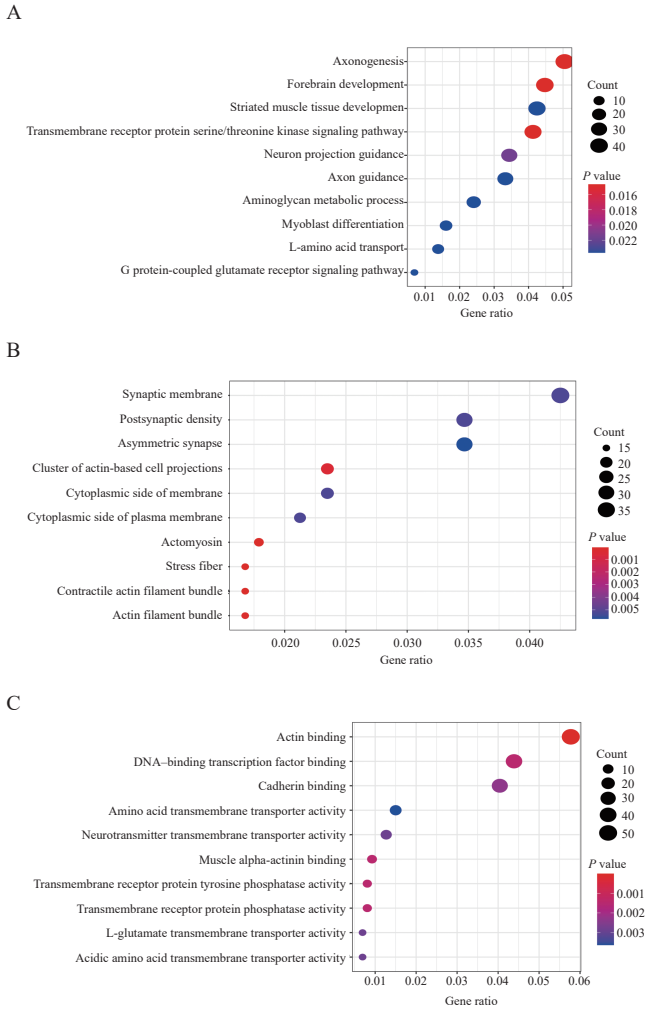

Figure 6 The top 10 GO enrichment of DMPs in CHD-induced unstable angina pectoris with Qi deficiency and blood stasis syndrome

A, the top 10 GO BP enrichment. B, the top 10 GO CC enrichment. C, the top 10 GO MF enrichment.

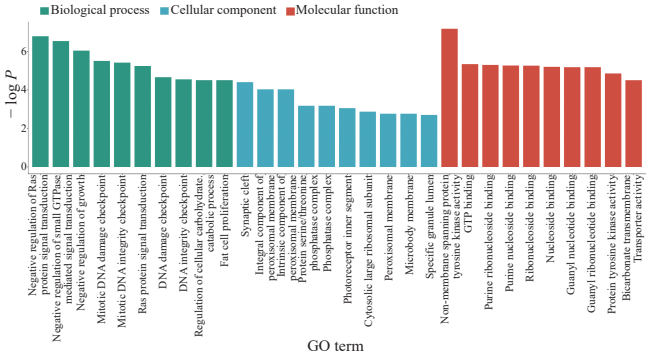

Figure 7 The top 10 GO enrichment of DMRs associated with CHD-induced unstable angina pectoris

3.5.4 GO enrichment analysis of DMRs associated with Qi deficiency and blood stasis syndrome in CHD-induced unstable angina pectoris In comparison between case and control groups, DMRs-associated genes were mainly involved in BP such as positive regulation of transmembrane transport, regulation of fatty acid metabolic process, and synaptic vesicle priming. Regarding CC, the genes were associated with Z disc, I band, and oligosaccharide transferase complex. In terms of MF, the genes were related to copper ion binding, mismatch repair complex binding, The receptor for advanced glycation end products (RAGE) binding. The top 10 entries for each GO category based on *P* value are presented in Figure 8.

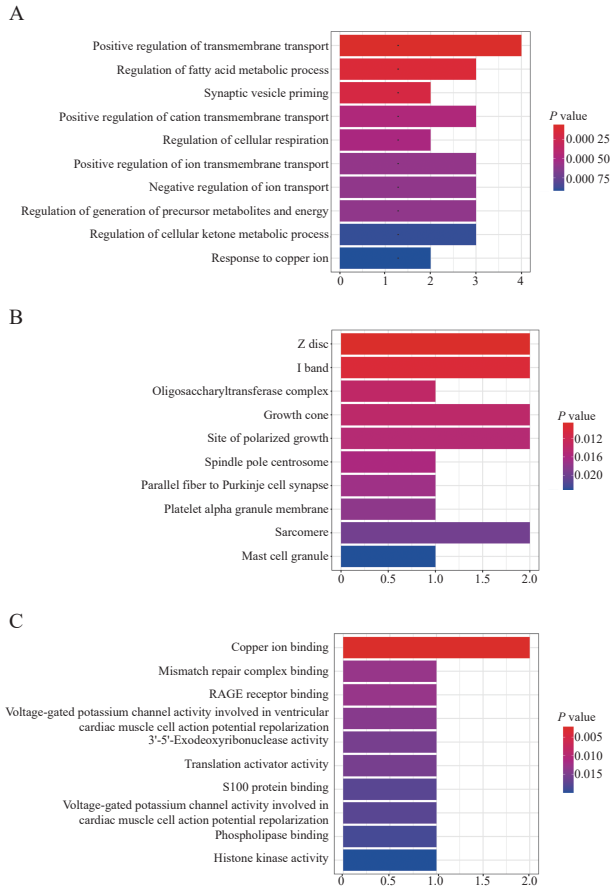

Figure 8 The top 10 GO enrichment of DMRs in CHD-induced unstable angina pectoris with Qi deficiency and blood stasis syndrome

A, the top 10 GO BP enrichment. B, the top 10 GO CC enrichment. C, the top 10 GO MF enrichment.

3.6 KEGG pathway enrichment analysis

3.6.1 KEGG pathway enrichment analysis of DMPs in CHD-induced unstable angina pectoris KEGG is a database resource for understanding molecular-level information on advanced functions and biological systems (such as cells, organisms, and ecosystems). In this study, genes associated with DMPs between G and J groups collectively mediated 159 pathways. Among these, significantly different pathways included fatty acid elongation, fatty acid metabolism, and endocytosis ($P < 0.05$) (Figure 9).

3.6.2 KEGG pathway enrichment analysis of DMPs associated with Qi deficiency and blood stasis syndrome in CHD-induced unstable angina pectoris Compared with control group, genes associated with DMPs mediated 17

significantly different signal pathways in case group ($P < 0.05$). The main pathways included endocytosis, Rap1 signaling pathway, glutamatergic synapse, axon guidance, insulin signaling pathway, and adenosine 5'-monophosphate (AMP)-activated protein kinase (AMPK) signaling pathway, as shown in Figure 10.

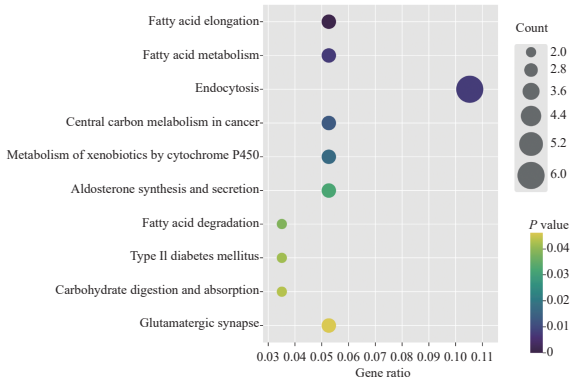

Figure 9 The top 10 KEGG enrichment of DMPs associated with CHD-induced unstable angina pectoris

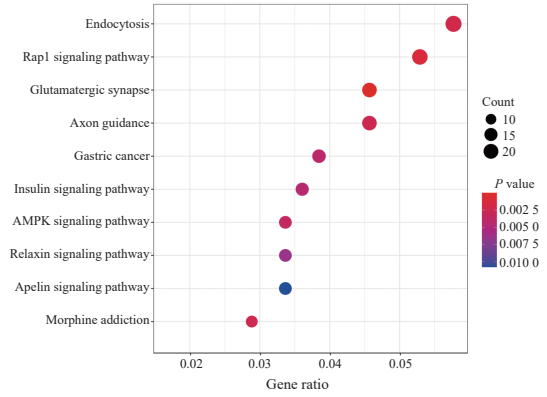

Figure 10 The top 10 KEGG enrichment of DMPs in CHD-induced unstable angina pectoris with Qi deficiency and blood stasis syndrome

4 Discussion

DNA methylation, a modification occurring on DNA sequences, stands as one of the most extensively researched and feature-rich epigenetic marks in the human genome. In vertebrates, DNA methylation typically entails the addition of a methyl group to the cytosine residue of CpG dinucleotide sequences (CpG sites), resulting in the formation of 5mC. This modification is crucial for gene expression, splicing, and stability. In somatic mammalian cells, the majority of CpG sites undergo methylation. However, CpG sites located in regions characterized by high CG content, referred to as CpG islands, often exhibit low levels of methylation [17].

Increasing evidence suggests a strong connection between DNA methylation and cardiovascular diseases [18, 19]. Global DNA methylation studies have revealed significantly higher levels of DNA methylation in patients with CHD compared with healthy individuals [20, 21]. Here, we employed the 850K methylation chip. Similar to previous research findings, we observed differences in DNA methylation expression between patients with CHD-induced unstable angina pectoris and the healthy controls. This further confirms the involvement of DNA methylation in the occurrence and development of CHD, providing new methylation patterns for the disease.

4.1 Hypermethylated DMPs associated with the "disease"

In this study, a total of 263 DMPs associated with the "disease" were identified. Among the hypermethylated sites, cg05845204 mapped to the RNA binding motif protein 39 gene (*RBM39*). Studies have found that *RBM39* [22] regulates cellular metabolism by co-initiating transcription through estrogen receptor α (ER-α) and nuclear factor κB (NF-κB), promoting the expressions of mitochondrial proteins and transcriptional regulator Myc-like (c-Myc) [23]. This leads to enhanced cartilage function, increased glucose metabolism, and supported cell growth and proliferation. Additionally, *RBM39* might contribute to cellular resistance against oxidative stress generated by metabolic reactions and exhibit autophagy-like phenotypes [23]. The site cg08906898 mapped to *ACAA2*, which is found to co-localize with Bcl-2 family BH3-only subunit (*BNIP3*) in mitochondria. It was reported that *ACAA2* was able to counteract *BNIP3*-induced apoptosis and inhibit apoptosis in human liver cancer HepG2 cells and osteosarcoma U-2 OS cells. This suggested that *ACAA2* functioned as a functional *BNIP3* binding partner, providing a potential link between fatty acid metabolism and apoptosis [24]. However, its expression and function in CHD still remain unclear.

4.2 Hypomethylated DMPs associated with the "disease"

Multiple hypomethylated sites, including cg26919182, map to the protein phosphatase 1 regulatory subunit 12B (*PPP1R12B*), also known as Myosin phosphatase targeting subunit 2 (*MYPT2*). *MYPT2* is a component of myosin light chain phosphatase (MLCP) and plays a regulatory role in muscle contraction. It exhibits specificity in the heart, skeletal muscles, and brain, influencing the sensitivity of Ca^{2+} in the contraction components of vascular smooth muscle cells. It was reported that the cardiac-specific myosin light chain phosphatase small subunit 21-kDa isoform (hHS-M21) encoded by *MYPT2* increased contraction in pig renal arteries and rat myocardium under constant Ca^{2+} concentration [25], overexpression of hHS-M21 was linked to impaired cardiac function and conduction abnormalities [26], providing strong evidence for studying the role of *MYPT2* in vascular constriction and cardiac dysfunction in CHD patients. However, the specific mechanisms of the action still require further exploration.

4.3 DMPs associated with the "sydrome"

Biological research on TCM syndromes is an unavoidable and crucial scientific issue [27]. In recent years, many TCM researchers have attempted to study the biological markers of TCM syndromes from the perspective of DNA methylation, thereby having uncovered the DNA methylation biological basis for TCM syndrome interpretation. DNA methylation studies related to CHD syndromes often focus on the methylation levels of specific genes, such as glycoprotein VI (*GP6*), angiotensin type 1 receptor-associated protein (*AGTRAP*), estrogen receptor β (*ER-*β) [28], interleukin 6 (*IL-6*) [29], thrombomodulin (*TM*) [30], and matrix metallopeptidase 9 (*MMP-9*) [31]. However, only a handful reports centered on syndrome research in CHD based on genome-wide DNA methylation. In this study, we pioneered the use of the 850K methylation chip to explore the differential expression profiles of DNA methylation in CHD-induced unstable angina pectoris patients with Qi deficiency and blood stasis syndrome compared with those without the syndrome, aiming to identify biological markers of the syndrome throughout the genome.

4.3.1 Hypermethylated DMPs associated with the "syndrome" In this study, a total of 1 703 DMPs related to "syndrome" were screened out. Among them, the hypermethylated site cg05573767 was mapped to the *RPS6KA2* gene, which encoded a member of the ribosomal S6 kinase (RSK) family of serine/threonine kinases. The protein's activity is related to the control of cell growth and differentiation. p38 mitogen-activated protein kinase (MAPK) is considered a focal or common pathway in various extracellular signal transduction pathways that lead to cell proliferation, hypertrophy, and apoptosis. It is involved in various stimuli-induced cardiac hypertrophy, proliferation, and apoptosis. Inhibiting poly (ADP-ribose) polymerase (PARP)/p53 and p38 MAPK expressions could alleviate oxidative stress and inflammatory reactions in a porcine CHD model [32].

4.3.2 Hypomethylated DMPs associated with the "syndrome" The hypomethylated site cg19938535 was mapped to the *LRRC16A* gene, also known as capping protein regulator and myosin 1 linker 1 (*CARMIL1*), which mediated cell migration and adhesion. Studies have shown that the RNAi-mediated knockdown of *CARMIL1* or its expression in a low level can inhibit actin assembly in the lipid layer, leading to its extreme structure distortion and affecting vascular permeability in atherosclerosis [33, 34]. The cg03893872 hypomethylated site was mapped to the *HHAT* gene, which encoded hedgehog acyltransferase. The hedgehog signaling pathway was considered a major pathway in morphogenesis and played a crucial role in embryonic development [34]. *HHAT* is regulated in a transforming growth factor-beta (TGF-β)-dependent manner in systemic sclerosis by activating TGF-β-induced hedgehog signaling pathway, thus promoting fibroblast activation and tissue fibrosis, while the inhibition of hedgehog signaling pathway plays an effective anti-fibrotic role in preclinical systemic sclerosis models [35]. However, further research is needed to understand the impact of the genes mapped by differentially methylated sites on TCM syndromes.

4.4 GO and KEGG enrichment analysis of DMPs associated with the "disease" and "syndrome"

In this study, GO enrichment analysis demonstrated that differentially methylated sites were mainly involved in BP such as transmembrane receptor protein serine/threonine kinase signaling pathways. They also affected CC like stress fibers and contractile actin filament bundles. Additionally, they were associated with MF such as actin binding. The KEGG pathway analysis revealed enrichment in pathways such as the Rap1 signaling pathway, AMPK signaling pathway, and insulin signaling pathway. The Rap1 signaling pathway played a crucial role in cardiovascular diseases, involving the regulation of integrins and cadherins, influencing adhesion and signal transduction [36]. Rap1 was essential for maintaining vascular endothelial homeostasis during development, as the loss of both required subtypes in endothelial cells led to embryonic lethality due to cardiovascular defects [37]. It was reported that in a mouse model of atherosclerosis, the loss of endothelial Rap1B exacerbated atherosclerotic plaque formation in the thoracic aorta, diminishing the anti-atherosclerotic effects of laminar shear stress-induced nitric oxide (NO) [38]. These findings can provide references for exploring molecular mechanisms.

4.5 DMRs profile of "disease" and "syndrome"

DMRs are considered to play a crucial role in regulating gene imprinting. In this study, we identified 23 DMRs associated with the "disease" category and 21 DMRs associated with the "syndrome" category. The overlapping gene in the DMR is *MUC4*, which encodes a membrane glycoprotein on the cell surface. *MUC4* can induce vascular generation through nuclear translocation, and its variation is not only present in CpG islands but also exhibits a regulatory relationship in methylation quantitative trait locus (meQTL). The methylation level of the *MUC4* was critical for CHD [39]. The specific function of recombinant ring finger protein 39 (*RNF39*) *in vivo* is yet to be clarified, but its position in the chromosome [surrounded by human leukocyte antigen (*HLA*) genes] suggests a potential role in immune responses. One study suggested that the loss of *RNF39* function might reduce the risk of endothelial plaque formation in coronary microvessels, rendering this gene a potential genetic locus related to CHD [40]. GO analysis revealed involvement in BP such as positive

regulation of transmembrane transport and regulation of fatty acid metabolic processes. CC included Z disc, I band, and oligosaccharicde transferase complex. MF encompassed copper ion binding, wherein copper ion binding plays a biological role through protein toxicity stress-induced cellular responses and toxic outcomes.

4.6 Significance and limitations of the study

In summary, this study has preliminarily established the differential DNA methylation expression profile of “disease” and “syndrome” in CHD-induced unstable angina pectoris patients with Qi deficiency and blood stasis. It has provided a foundation for the integration of TCM syndromes. However, the study still has some limitations, such as small sample size, inclusion of only unstable angina pectoris patients, relatively limited pattern stratification, and data interpretation being susceptible to different calculation methods. Future research should focus on expanding clinical sample sizes, conducting multicenter, large-scale, and in-depth studies, and validation. Additionally, leveraging bioinformatics techniques comprehensively, interpreting data from various dimensions, such as “same disease with different syndromes” and “different diseases with same syndrome”, will help explore a more comprehensive biological basis reflecting the essence of “disease” and “syndrome”. This research hopes to contribute to a more thorough understanding of the pathogenesis of CHD and its relationship with syndromes in TCM.

5 Conclusion

This study reveals the methylation patterns of DMPs and DMRs in patients with Qi deficiency and blood stasis syndrome caused by CHD-induced unstable angina pectoris. Potential epigenetic regulation of fatty acid metabolism, Rap1 signaling, and other molecular functions are involved in the development of CHD between the "disease" and "syndrome". Further validation studies are needed to confirm the generalizability of these findings and assess their potential as clinical biomarkers or therapeutic targets for the prevention and treatment of CHD with Qi deficiency and blood stasis syndrome.

Fundings

Natural Science Foundation of Hunan Province (2022JJ40287), Excellent Youth Program of Hunan Education Department (21B0081), Hunan Provincial Administration of Traditional Chinese Medicine (D2022027), and Natural Science Foundation of Changsha (kq2202255).

Competing interests

The authors declare no conflict of interest.

References

[1] RIZZACASA B, AMATI F, ROMEO F, et al. Epigenetic modification in coronary atherosclerosis: JACC review topic of the week. Journal of the American College of Cardiology, 2019, 74(10): 1352–1365.

[2] ZHAO D, LIU J, WANG M, et al. Epidemiology of cardiovascular disease in China: current features and implications. Nature Reviews Cardiology, 2019, 16(4): 203–212.

[3] The Writing Committee of the Report on Cardiovascular Health Diseases in China. Interpretation of Report on Cardiovascular Health and Diseases in China 2021. Chinese Journal of Cardiovascular Medicine, 2022, 27(4): 305–318.

[4] PLUTZKY J. Epigenetic therapeutics for cardiovascular disease: writing, erasing, reading, and maybe forgetting. JAMA, 2020, 323(16): 1557–1558.

[5] LIPPI G, CERVELLIN G. The interplay between genetics, epigenetics and environment in modulating the risk of coronary heart disease. Annals of Translational Medicine, 2016, 4(23): 460.

[6] GREENBERG MVC, BOURC'HIS D. The diverse roles of DNA methylation in mammalian development and disease. Nature Reviews Molecular Cell Biology, 2019, 20(10): 590–607.

[7] WANG X, LIU AH, JIA ZW, et al. Genome-wide DNA methylation patterns in coronary heart disease. Herz, 2018, 43(7): 656–662.

[8] DUAN L, HU JY, XIONG XJ, et al. The role of DNA methylation in coronary artery disease. Gene, 2018, 646: 91–97.

[9] WANG CC, WU SHAN, JIANG LJ, et al. Research situation of traditional Chinese medicine clinical epidemiological investigation of coronary heart disease in China from 1990 to 2020. Chinese Journal of Basic Medicine in Traditional Chinese Medicine, 2020, 26(12): 1883–1893.

[10] BI YF, WANG XL, MAO JY, et al. Recommendations for the diagnosis of coronary heart disease and angina pectoris TCM syndromes based on clinical epidemiological investigation. Journal of Traditional Chinese Medicine, 2018, 59(22): 1977–1980.

[11] LI XJ, CHEN JX, LIU YY. Discussion about the significance of TCM syndrome biological foundation in the improvement of TCM syndrome differentiation system. China Journal of Traditional Chinese Medicine and Pharmacy, 2017, 32(6): 2353–2357.

[12] KE YN, CHEN YL. Guidelines for the diagnosis and treatment of unstable angina and non-ST-segment elevation myocardial infarction. Chinese Journal of Cardiovascular Medicine, 2007, 35(4): 295–304.

[13] GE JB, XU YJ. Internal medicine. 8th ed. Beijing: People’s medical, 2013.

[14] WANG J, LI J, MAO JU, et al. Syndrome differentiation and diagnostic criteria for the main syndrome types of coronary heart disease and angina pectoris. Chinese Journal of Integrated Traditional and Western Medicine, 2018, 38(2): 154–155.

[15] SOLOMON O, MACISAAC J, QUACH H, et al. Comparison of DNA methylation measured by Illumina 450K and EPIC BeadChips in blood of newborns and 14-year-old children. Epigenetics, 2018, 13(6): 655–664.

[16] LEE MK, XU CJ, CARNES MU, et al. Genome-wide DNA

methylation and long-term ambient air pollution exposure in Korean adults. Clinical Epigenetics, 2019, 11(1): 37.

[17] JONES PA. Functions of DNA methylation: islands, start sites, gene bodies and beyond. Nature Reviews Genetics, 2012, 13(7): 484–492.

[18] ZHANG J, KAI LI, LIAO DF. Application of Nuc-mtDNA and DNA methylation analysis in life science and medical studies. Digital Chinese Medicine, 2022, 5(3): 233–235.

[19] CHILUNGA FP, HENNEMAN P, VENEMA A, et al. Genome-wide DNA methylation analysis on C-reactive protein among Ghanaians suggests molecular links to the emerging risk of cardiovascular diseases. NPJ Genomic Medicine, 2021, 6(1): 46.

[20] AGHA G, MENDELSON MM, WARD-CAVINESS CK, et al. Blood leukocyte DNA methylation predicts risk of future myocardial infarction and coronary heart disease. Circulation, 2019, 140(8): 645–657.

[21] SHARMA P, KUMAR J, GARG G, et al. Detection of altered global DNA methylation in coronary artery disease patients. DNA and Cell Biology, 2008, 27(7): 357–365.

[22] XU YW, NIJHUIS A, KEUN HC. RNA-binding motif protein 39 (RBM39): an emerging cancer target. British Journal of Pharmacology, 2022, 179(12): 2795–2812.

[23] KANG YK, PUTLURI N, MAITY S, et al. CAPER is vital for energy and redox homeostasis by integrating glucose-induced mitochondrial functions via ERR-α-Gabpa and stress-induced adaptive responses via NF-κB-cMYC. PLoS Genetics, 2015, 11(4): e1005116.

[24] CAO W, LIU NS, TANG S, et al. Acetyl-Coenzyme A acyltransferase 2 attenuates the apoptotic effects of *BNIP3* in two human cell lines. Biochimica et Biophysica Acta, 2008, 1780(6): 873–880.

[25] SHICHI D, ARIMURA T, ISHIKAWA T, et al. Heart-specific small subunit of myosin light chain phosphatase activates rho-associated kinase and regulates phosphorylation of myosin phosphatase target subunit 1. The Journal of Biological Chemistry, 2010, 285(44): 33680–33690.

[26] ARIMURA T, MUCHIR A, KUWAHARA M, et al. Overexpression of heart-specific small subunit of myosin light chain phosphatase results in heart failure and conduction disturbance. American Journal of Physiology Heart and Circulatory Physiology, 2018, 314(6): H1192–H1202.

[27] ZHOU XY, YANG SW, OU JT, et al. Screening influencing factors of blood stasis constitution in traditional Chinese medicine. Digital Chinese Medicine, 2022, 5(2): 169–177.

[28] TANG MS. Research into relationship between estrogen receptor gene β promoter region methylation status and blood stasis syndrome of premature coronary heart disease. China Journal of Traditional Chinese Medicine and Pharmacy, 2015, 30(5): 1464–1468.

[29] CHEN G, HE HQ, LIU YM, et al. IL-6 gene promoter methylation in patients with blood stasis syndrome and unstable angina. Chinese Journal of Experimental Traditional Medical Formulae, 2017, 23(19): 23–27.

[30] LI Y. Effects of integrated traditional Chinese and western medicine treatment on plasma *TM* gene promoter methylation in patients with ACS (phlegm and blood stasis type). Shenyang: Liaoning University of Traditional Chinese Medicine, 2019.

[31] CHI YX. Effects of integrated traditional Chinese and western medicine treatment on *MMP-9* gene promoter methylation levels in ACS patients with phlegm, turbidity and blood stasis. Liaoning University of Traditional Chinese Medicine, 2019.

[32] YANG B, XU B, ZHAO H, et al. Dioscin protects against coronary heart disease by reducing oxidative stress and inflammation via Sirt1/Nrf2 and p38 MAPK pathways. Molecular Medicine Reports, 2018, 18(1): 973–980.

[33] LIANG Y, NIEDERSTRASSER H, EDWARDS M, et al. Distinct roles for CARMIL isoforms in cell migration. Molecular Biology of the Cell, 2009, 20(24): 5290–5305.

[34] INGHAM PW, MCMAHON AP. Hedgehog signaling in animal development: paradigms and principles. Genes & Development, 2001, 15(23): 3059–3087.

[35] LIANG RF, KAGWIRIA R, ZEHENDER A, et al. Acyltransferase skinny hedgehog regulates TGFβ-dependent fibroblast activation in SSc. Annals of the Rheumatic Diseases, 2019, 78(9): 1269–1273.

[36] CHRZANOWSKA-WODNICKA M. Rap1 in endothelial biology. Current Opinion in Hematology, 2017, 24(3): 248–255.

[37] GAONAC'H-LOVEJOY V, BOSCHER C, DELISLE C, et al. Rap1 is involved in angiopoietin-1-induced cell-cell junction stabilization and endothelial cell sprouting. Cells, 2020, 9(1): 155.

[38] SINGH B, KOSURU R, LAKSHMIKANTHAN S, et al. Endothelial Rap1 (ras-association proximate 1) restricts inflammatory signaling to protect from the progression of atherosclerosis. Arteriosclerosis, Thrombosis, and Vascular Biology, 2021, 41(2): 638–650.

[39] WANG J, MA XQ, ZHANG Q, et al. The interaction analysis of SNP variants and DNA methylation identifies novel methylated pathogenesis genes in congenital heart diseases. Frontiers in Cell and Developmental Biology, 2021, 9: 665514.

[40] WENG L, TAYLOR KD, CHEN YD, et al. Genetic loci associated with nonobstructive coronary artery disease in Caucasian women. Physiological Genomics, 2016, 48(1): 12–20.

冠心病不稳定型心绞痛气虚血瘀证“病”与“证”DNA 甲基化差异表达谱分析

吴华英[a], 胡宏春[a], 刘宇峰[a], 李亮[b], 李静[b], 韩育明[c], 肖长江[c*], 彭清华[b*]

a. 湖南师范大学医学院, 湖南 长沙 410013, 中国
b. 湖南中医药大学中医诊断学湖南省重点实验室, 湖南 长沙 410208, 中国
c. 湖南省中医药研究院附属医院心血管内科, 湖南 长沙 410006, 中国

【摘要】目的 探讨冠心病（CHD）所致不稳定型心绞痛气虚血瘀证患者外周血 DNA 甲基化位点/区域的差异表达谱及潜在分子机制，为冠心病病证结合研究提供科学依据。**方法** 根据预先确定的纳入和排除标准，将研究对象分为两组，即 CHD 诱发的不稳定型心绞痛组（G 组）和健康对照组（J 组），进行“病”分析，而不稳定型心绞痛患者进一步分为气虚血瘀证组（病例组）和非气虚血瘀证组（对照组）进行“证”分析。收集研究对象的一般资料和临床信息，空腹抽取外周静脉血，采用 850K 甲基化芯片检测各组 DNA 甲基化差异表达谱。使用 ChAMP 软件（V 2.14.0）进行差异甲基化数据分析，阈值为校正后 $P < 0.01$。采用基因本体论（GO）和京都基因组百科全书（KEGG）数据库对相关映射基因进行功能和通路富集分析。**结果** G 组和 J 组比较，得出代表“病”的差异甲基化表达谱，共筛选出 263 个差异甲基化位点（DMPs），其中包括 cg05845204、cg08906898 等 191 个高甲基化位点和 cg26919182、cg13149459 等 72 个低甲基化位点。这些位点主要映射到 148 个基因，包括 RNA 结合基序蛋白 39（*RBM39*）、乙酰辅酶 A 酰基转移酶 2（*ACAA2*）、蛋白磷酸酶 1 调节亚基 12B（*PPP1R12B*）和双特异性酪氨酸磷酸化调节激酶 2（*DYRK2*）。GO 功能富集分析结果显示 DMPs 基因主要富集于染色体蛋白质定位、细胞形态发生调控、钙介导信号负向调控等方面。KEGG 通路分析结果提示这些基因主要富集于脂肪酸代谢和内吞途径。此外，共鉴定出 23 个代表“病”的差异甲基化区域（DMRs），并识别出跨膜蛋白 232（*TMEM232*）、核糖体蛋白 P1（*RPLP1*）、过氧化物酶体发生因子 10（*PEX10*）和叉头蛋白 N3（*FOXN3*）等重叠基因，GO 功能主要富集于 Ras 蛋白信号转导的负向调节和小 GTP 酶介导的信号转导、负向调节等方面。病例组与对照组比较获得代表“证”的差异甲基化表达谱，共筛选出 1 703 个“证”相关 DMPs，包括 cg05573767 等 444 个甲基化升高位点和 1 259 个甲基化降低位点，例如 cg19938535 和 cg03893872。这些位点映射到 1 108 个基因，例如核糖体蛋白 S6 激酶 A2（*RPS6KA2*）、亮氨酸重复序列 16A（*LRRC16A*）和刺猬酰基转移酶（*HHAT*）。GO 功能富集分析，差异甲基化位点相关基因主要富集于跨膜受体蛋白丝氨酸/苏氨酸激酶信号通路、轴突发生等生物学功能。KEGG 通路富集分析结果提示 Rap1 信号通路、5′-单磷酸腺苷激活蛋白激酶（AMPK）等信号通路参与了证候发展。研究共筛选出 21 个“证”相关 DMRs，包括 22 个重叠基因，如粘蛋白 4（*MUC4*）、三素修复核酸外切酶 1（*TREX1*）和 LIM 同源盒 6（*LHX6*）。GO 富集分析发现主要参与正向调节跨膜转运、调节脂肪酸代谢和铜离子结合等分子功能。**结论** 本研究揭示了冠心病不稳定心绞痛气虚血瘀证患者 DMPs 和 DMRs 的甲基化特征，脂肪酸代谢、Rap1 信号通路和其他分子功能的潜在表观遗传调控参与了冠心病“病”和“证”的发展。

【关键词】冠心病；气虚血瘀证；不稳定型心绞痛；DNA 甲基化；表观遗传学；850K 甲基化芯片